



Effect of Inclination of Twin Jets Impinging a Heated Wall

F. Bentarzi ¹, A. Mataoui ^{1†} and M. Rebay ²

¹Theoretical and Applied Laboratory of Fluid Mechanics, Physics Faculty, USTHB, Algiers, Algeria
²GRESPI / Lab. de Thermomécanique- Université de Reims Champagne-Ardenne- 51687 Reims, France

†Corresponding Author Email: amataoui@usthb.dz

(Received March 9, 2018; accepted August 26, 2018)

ABSTRACT

This study examines the interaction of twin oblique turbulent slot-jets of different directions (divergent, convergent or parallel) impinging a heated wall. A comparison of the results is done between the cases of perpendicular jets and three cases of twinned jets (parallel, convergent and divergent). The twin slot jets are located on a confining adiabatic wall at a distance of 8 slot jet width. Convective heat is investigated numerically examining the effect of Reynolds number (Re) and jet inclination angle (α). This problem is relevant to a wide range of practical applications including nuclear engineering devices, manufacturing, material processing, electronic cooling, drying paper or textile, tempering of glass, etc. The numerical investigation is performed using two dimensional large eddy simulations (LES) approach with Smagorinsky sub-grid scale (SGS) models. The results show the presence of a complex flow resulting from the interaction of the two jets. When the impingement angle is reduced from 0° (perpendicular impingement) to 60° , the position of the stagnation points are modified and therefore the peaks of the Nusselt number locations on the impingement surface and their magnitude, vary. For largest Reynolds number Nusselt number is enhanced for all types of inclination. The averaged Nusselt number shows that the perpendicular impingement gives better heat transfer than that of the oblique jets. The poor heat transfer is obtained for the parallel oblique jets. For the same angle, divergent jets give smallest heat transfer than the convergent jets.

Keywords: Twin impinging jets; Heat transfer; Large Eddy Simulation; Oblique jets; Finite volume method.

NOMENCLATURE

C_p	pressure coefficient	X_{MP}	merging point location
D	distance between the jet exit to the wall	X_{CP}	combining point location
H	distance between the two jets	w	nozzle thickness
K	turbulent kinetic energy	ε	dissipation rate of turbulent energy
L	wall length	ν	viscosity kinematic
Nu	Nusselt number	ν_t	eddy viscosity
Pr	Prandtl number	ρ	fluid density
Re	Reynolds number	<i>Indices</i>	
T	mean temperature	1	first jet
U	mean velocity in x-axis direction	2	second jet
V	mean velocity in y-axis direction		
x_i	point coordinate		

1. INTRODUCTION

Since more than half a century, impinging jet heat transfer has been investigated in many studies. They can be easily introduced into industrial devices and often generate local improvements in heat and mass transfer. Turbulent impinging jets is a very effective techniques to enhance heat exchange that may be required in several applications include material processing, electronic cooling, drying paper or

textiles, tempering of glass, drying of paper and textiles, annealing of nonferrous metal sheets, and cooling of microelectronic components. Etc... A number of comprehensive reviews of single jet impingement are available in the literature review of Livingood and Hrycak (1973), Martin, H. (1977), Zuckerman and Lior (2005 and 2006) as well as Shukla and Dewan (2017). Relevant studies have been conducted numerically by many researchers of single impingement jet and have obtained a good

agreement with experiment data as [Wolfshtein \(1970\)](#), [Looney and Walsh \(1984\)](#), [Craft *et al.* \(1993\)](#), [Craft *et al.* \(1993\)](#), [Cooper *et al.* \(1993\)](#), [Baydar and Ozmen \(2005\)](#), [cho *et al.* \(2011\)](#), [Draksler and Končar \(2011\)](#), [Benmouhoub and Mataoui \(2013\)](#). It has been shown in the literature that the using of multijets impinging on a hot wall give better heat transfer over the target wall than single jet ([Rathee *et al.* \(2015\)](#)). An active control system using multijets with the ability to adapt time-varying flow fields has been developed by [Hasegawa and Kumagai \(2008\)](#). They found that of the present study are summarized as follows: the multijets may suppress the flow separation for flow fields. [Saad *et al.* \(1992\)](#), [Seyedein *et al.* \(1995\)](#), [Rady and Arquís \(2006\)](#), examined the heat transfer enhancement of multiple impinging slot jets. [Buchlin \(2011\)](#) found that in nozzle array systems the impinging distance and the nozzle- to-nozzle spacing control the jet-to-jet interaction. [Koched *et al.* \(2011\)](#), examined Vortex Structure in the Wall Region of an Impinging slot Jet. Twin jet flow field is characterized by three distinct regions, namely converging region, merging region and combined region. For twin slot jets impinging perpendicularly on a flat plate, different types of interactions are defined when the wall is located before, within and after the merging region. An improvement in heat transfer is generated by the interaction of the jets with each other before the impingement. The increase of turbulence kinetic energy occurs for high gradient velocity. The analysis reveals that the average Nusselt number increases considerably with the jet exit Reynolds number. Most previous studies have been devoted to the problems of perpendicular interactions of single or multiple jets with a solid wall. The inclination of twin jets is used in some engineering applications to control the location of the maximum heat transfer coefficient. Oblique jets impinging a solid wall were also topic of several researchers since they may play an important role in the expansion or reduction of the heat transfer area. A number of numerical and experimental studies were investigated for inclined circular jet impingement since these last decades ([Sparrow and Lovell \(1980\)](#), [Goldstein and Franchett \(1988\)](#), [Beitelmal *et al.* \(2000\)](#), [Tong \(2003\)](#), [Oztop *et al.* \(2011\)](#), [Parida *et al.* \(2011\)](#) and [Kito \(2012\)](#)). They concluded that the location of stagnation point and maximum heat transfer depend on the inclination angle of the jet and it plays an important role for higher Reynolds number. However, heat transfers by inclined slot jets impinging a surface have received a small interest compared to perpendicular impingement. The inclination of the slot jets which impinge a heated wall may also control heat transfer improvement.

Twin inclined jet flow field is also characterized by three distinct regions: converging, merging and combined regions. This configuration is qualitatively similar to that produced by twin perpendicular jets ([Wang, H *et al.* \(2016\)](#)). The resulting flow diffusion effect may prevent a targeted region to work continuously at high temperature. This cooling knowledge is predictable to involve main practical implications in controlled

space and large area electronic cooling. Furthermore, heat-transfer enhancement may be improved by jets inclination (α). Patel and Roy (2002) have studied numerically the effect of Reynolds number (Re) and jet inclination on the local and average heat transfer (Nu) and suggested some correlations for twin rectangular jets impinging an inclined surface.

The present study is the extension of previous works by RANS first and second order turbulence modelling ([Bentarzi *et al.* 2009](#), [Nouali and Mataoui \(2014\)](#) and [Bentarzi *et al.* 2014](#)), to inclined impinging jets. Four interactions (perpendicular, divergent, convergent and parallel) of the two jets impinging a hot wall are studied in order to find the configuration that would give the best heat transfer rate. The schematic descriptions of these configurations are summarized in Fig. (1).

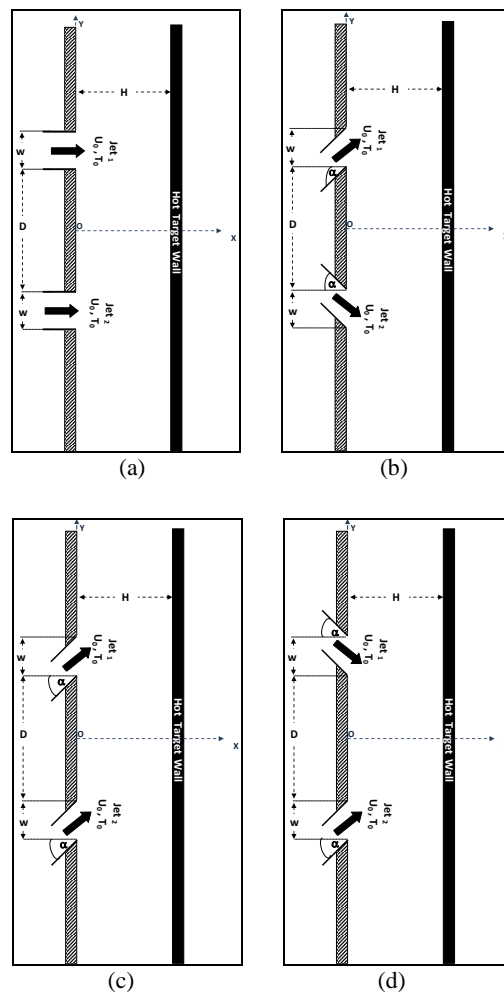


Fig. 1. Twin-jets flow configuration (a) Perpendicular (b) Divergent (c) Parallel (d) Convergent.

The jets are isothermal fully developed turbulent at the exit of the nozzles and the plate is heated uniformly. All the geometric lengths are normalized by the thickness of the slot, w , which for two dimensional configurations with infinite span is half the jet hydraulic diameter. The separation distance between the nozzles and the target plate is H and

the distance of separation between the inner edges of the twin slot jets is D . The large eddy simulation is used for the computations. This configuration has been involved in several works for its interesting applications in heat transfer phenomena.

2. METHODOLOGY

2.1 Governing Equations

The flow is considered fully turbulent of Newtonian and incompressible fluid with constant thermo physical properties. The averaged equations in Cartesian coordinates are deduced from the mass, momentum and energy balance coupled with the equations of the turbulent quantities as follows:

Mass conservation equation:

$$\frac{\partial U_i}{\partial x_i} = 0 \quad (1)$$

Momentum conservation equation:

$$\frac{\partial U_i}{\partial t} + \rho U_j \frac{\partial U_i}{\partial x_j} = -\frac{\partial P}{\partial x_i} + \frac{\partial}{\partial x_j} \left(\mu \frac{\partial U_i}{\partial x_j} - \rho u_i u_j \right) \quad (2)$$

Energy conservation equation:

$$\frac{\partial T}{\partial t} + \rho U_i \frac{\partial T}{\partial x_i} = \frac{\partial}{\partial x_i} \left(\frac{\mu}{Pr} \frac{\partial T}{\partial x_i} - \rho u_i \theta \right) \quad (3)$$

Where P , T and U_i are the mean pressure, temperature and velocity components respectively. Here θ and u_i are the temperature and velocity components fluctuations, respectively and x_i is the space coordinates. The fluid properties ρ , μ and Pr are respectively the density, the dynamic viscosity and the Prandtl number. In this paper, the closure of the equations is achieved using large eddy dissipation model (LES).

LES approach is a time-dependant simulation technique which aims at properly resolving large coherent and anisotropic structures of the flow. The turbulent viscosity is estimated using the model of Smagorinsky (1964), and is supposed to be proportional to a subgrid characteristic length scale (Smagorinsky 1964). Navier-Stokes equations are filtered in space by using Large Eddy Dissipation turbulence model, which gives rise to subgrid scales (SGS) Reynolds stress needing modelling.

The SGS model is coupled with the Boussinesq hypothesis to compute the subgrid stress τ_{ij} defined as:

$$\tau_{ij} - \frac{2}{3} \tau_{kk} \delta_{ij} = -2\mu_t \overline{S_{ij}} \quad (4)$$

Where μ_t is the SGS turbulent viscosity, τ_{kk} the isotropic component of the SGS stress, and $\overline{S_{ij}}$ the rate of strain of the resolved scale which is given by:

$$\overline{S_{ij}} = \frac{1}{2} \left(\frac{\partial \overline{u_i}}{\partial x_j} + \frac{\partial \overline{u_j}}{\partial x_i} \right) \quad (5)$$

In the Smagorinsky SGS approach [6], the eddy viscosity is modelled as:

$$\mu_t = \rho L_s^2 \left| \overline{S} \right| \quad (6)$$

where L_s is the SGS mixing length and the strain rate magnitude $\left| \overline{S} \right|$ is defined by:

$$\left| \overline{S} \right| \equiv \sqrt{2 \cdot \overline{S_{ij}} \cdot \overline{S_{ij}}} \quad (7)$$

while L_s is given by:

$$L_s = \min(\kappa d, C_s \Delta) \quad (8)$$

In the above, κ is Von Karman constant, d the distance to the nearest wall, C_s the Smagorinsky coefficient and Δ the local spatial scale, which in the Fluent implementation is taken to be the cell volume to the power one third in 3D (or to the power one half in 2D). In the classical Smagorinsky SGS model (Smagorinsky (1964)), C_s is taken to be a constant around 0.1. It has been shown however that assuming C_s to be a constant leads to excessive damping of large scale fluctuations. Hence, Germano (1991) and later Lilly (1992) have outlined a dynamic procedure based on multiple spatial filtering in order to deduce a local, more universal value for C_s .

The filtered energy equation can be written by:

$$\rho C_p \frac{\partial T}{\partial t} + \rho C_p U_i \frac{\partial T}{\partial x_i} = \frac{\partial}{\partial x_i} \left(\Gamma C_p \frac{\partial T}{\partial x_i} - q_j^{SGS} \right) \quad (9)$$

$$q_j^{SGS} = -\Gamma_{SGS} C_p \frac{\partial T}{\partial x_j}$$

q_j^{SGS} is the sub-grid scale heat flux, which is modelled by a standard gradient diffusion model

2.2 Numerical Procedure

The numerical predictions based on finite volume method are performed by ANSYS FLUENT 14.0 CFD code. The discretization of each transport equation is done on collocated meshes. The algorithm SIMPLE (Patankar, 1981) is used for pressure-velocity coupling. A bounded central differencing was achieved for spatial discretization and the second order implicit scheme is used for temporal integration. For each calculation, the time step is chosen so that the courant number is less or equal to 1 in the whole calculation domain. The solution is considered converged when the normalized residual of each variable is less than 10^{-9} . Boundary conditions for this flow configuration include the inflow (inlet), solid wall and outlet as shown in Fig. 1.

- At each jet exit, constant parameters are imposed. Velocity components depend on the interaction type, as follows:

Perpendicular interaction: $U_1= U_2= +U_0$ and $V_1= V_2= 0$

Convergent interaction: $U_1= U_2= +U_0 \cos(\alpha)$ and $V_1= -U_0 \sin(\alpha)$, $V_2= +U_0 \sin(\alpha)$

Divergent interaction: $U_1= U_2= +U_0 \cos(\alpha)$ and $V_1= +U_0 \sin(\alpha)$, $V_2= -U_0 \sin(\alpha)$

Parallel interaction: $U_1= U_2= +U_0 \cos(\alpha)$ and $V_1= +U_0 \sin(\alpha)$, $V_2= +U_0 \sin(\alpha)$

Both jets are at ambient temperature T_0

For each jet turbulent intensity I_0 is of 2% and their dissipation rate is deduced from the macro-scale of turbulence corresponding to jet thickness; which is defined in terms of k , ϵ and the modeling constant $c_{\mu}^{3/4}$ ($C_{\mu}=0.09$) (Launder and Spalding (1972)) as follows :

$$k = \frac{3}{2}(U_0 I_0)^2 \text{ and } \epsilon = C_{\mu} \frac{(k)^{3/2}}{0.03w}, I = 0.02$$

- At the outlet, the static pressure and temperature are kept respectively at atmospheric pressure and ambient temperature. The relative static pressure at these boundaries was set to zero; assumed as reference of atmospheric value. The free boundaries are far from the flow interaction in order to avoid their influences on the numerical solution.

- All the walls of the configuration are impermeable. At solid walls: the no-slip boundary condition is applied; where all dynamical variables are set to zero. For temperature, the impinging wall is heated at constant temperature $T_w > T_0$ and the confining walls are adiabatic.

A two dimensional structural non uniform grid has been generated. A sufficiently fine grid is generated near the jet and the wall where a very high gradient of each variable prevails. Large Eddy Dissipation model requires a fine grid size perpendicular to the wall, thus, the boundary layer near the surface was kept in order of $x^+ < 1$.

A systematic grid independence tests are performed to obtain the required mesh resolution. The distribution of the local Nusselt number and pressure coefficient along the impingement wall for different grids refinement is shown in Fig. 2 for a perpendicular twin-jet configuration at Re 50000. This figure confirms that there are no significant variations for local Nusselt number Nu and pressure coefficient for refinements beyond 42300 cells. Thus, this grid is used for all calculations of all configurations (perpendicular, divergent, convergent and parallel interactions), since the size of the computational domain has not been modified ($H = 8w$ and $D = 20w$).

For the validation, we do not find experimental results for the case of a twin jet impinging a solid wall, for this we have validated this numerical method and turbulence model with the experimental results of single jet (Fig. 3). A good agreement is obtained with experimental data of Gardon and Akfirat (1966) for the case of $D/W=8$ and

Re=11000 (Fig. 3).

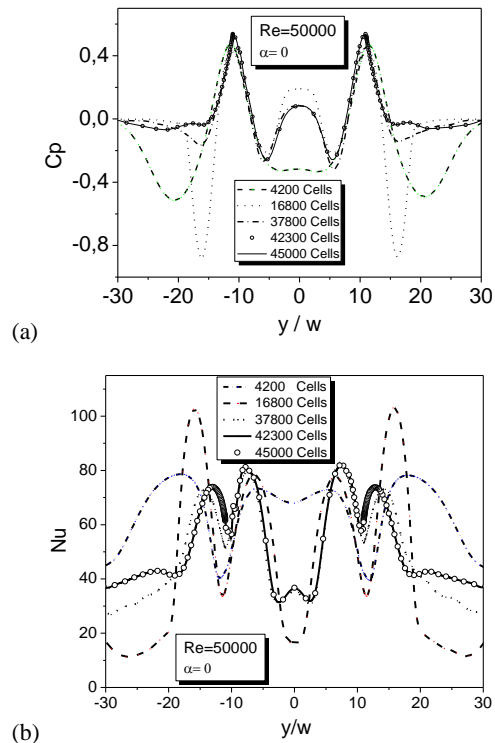


Fig. 2. Typical grid test (Re=50000, $\alpha=0$) (a) Pressure coefficient (b) Local Nusselt number.

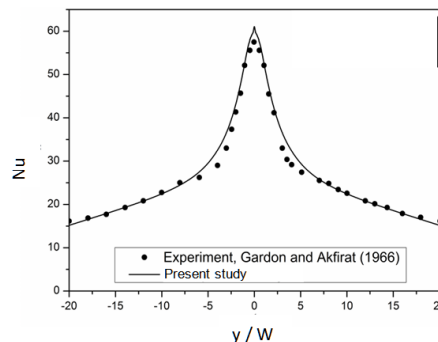


Fig. 3. Validation of Numerical Procedure ($D/w=8$ and $Re=11000$).

3. RESULTS AND DISCUSSIONS

The present work investigated numerically the flow structure and heat transfer characteristics of twin slot inclined jet impinging an isothermal hot wall. Both velocity and temperature fields are calculated. Both jets are inclined in different directions in order to find the best heat transfer. Four configurations are checked: Perpendicular, Convergent, Parallel and Divergent (Fig. 1). The impinging distance D and the distance between the jets are respectively set at $8w$ and $20w$, and the parameters of the problem which have been examined are: the Reynolds number (Re, on the basis of the thickness of the nozzle between 11000 and 50000) and the inclination of the jets which has been varied from 0° to 60° for all

interactions types (Perpendicular, Convergent, Divergent and Parallel).

3.1 Flow Structure

Further computations are done by varying the impingement angle; they show that the flow field is characterized by the formation of multiple recirculation bubbles in the domain for each type of interaction. The jets impinge the target hot surface and exit toward each outlet of the domain. Several eddies are formed between the two walls. The size and the shape of each eddy are related to the type of interaction. The flow structure is examined for the case $11000 \leq Re \leq 50000$, $D/w=8$, $H/w=20$ and $0 \leq \alpha \leq \pi/6$ for oblique jets. For more clarity the streamlines contours are illustrated for each interaction type in Fig. 4 (a, b, c and d) for $Re=50000$ and $\alpha=\pi/6$. Convergent, perpendicular and divergent interactions are symmetrical and characterized by several eddies. The size of the two main eddies between the two jets depend on the type of interaction. The largest eddies are obtained for divergent interaction, this results have been confirmed by Sharif *et al.* (2015). However, these eddies are compressed for the convergent interaction in comparison of the case of perpendicular interaction. On the other hand, the parallel interaction is asymmetric. So, we can confirm that the perpendicular velocity component V can control the size of vortices, thus the location of the stagnation points. The corresponding isobars computed through mean static pressure. Perpendicular interaction is characterized by four areas of negative pressure of significant magnitude. The other interactions are characterized by two main negative area of great magnitude by Coanda effect. This fact may be explained by the effect of the normal velocity of all oblique interactions. Along the impinging wall, there are three areas of positive pressure, for all interactions.

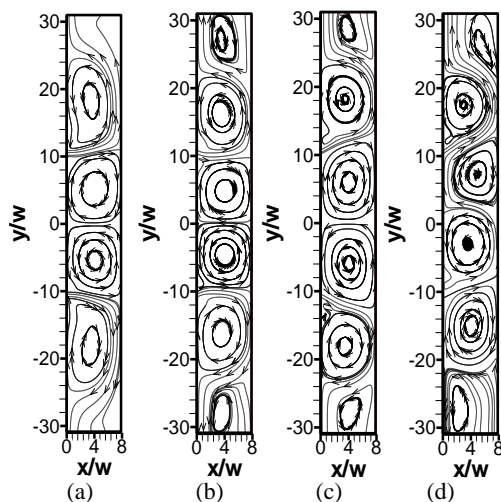


Fig. 4. Streamlines contours $Re=50000$, $H/w=20$, $D/w=8$ and $\alpha=\pi/6$ for oblique jet (a) Perpendicular, (b) Convergent, (c) Divergent and (d) Parallel.

3.2 Pressure Coefficient

For each type of interaction, Figs. 5 and 6 depict a comparison of the static pressure distribution along the hot wall for several inclination and different Reynolds number. We notice that the pressure coefficients exhibit the same shape for each Reynolds number. These figures highlight that two sub atmospheric regions on the impingement plate. All curves have a symmetrical shape for perpendicular, convergent and divergent jets interactions, and asymmetric shape for parallel interaction. The maximum corresponds to the location of the stagnation point and depends on inclination angle and the type of interaction. Beyond that, the pressure coefficient decreases on both sides of each jet. Two behaviors are observed depending on inclination ranges. For each interaction type, the locations of the stagnation points are affected significantly by the inclination of the jets. For $0 \leq \alpha \leq \pi/4$ symmetrical interactions (perpendicular, convergent or divergent), Reynolds number has a minor effect on the pressure coefficient, whereas it modifies considerably the trend of the cp profile for parallel interaction (Fig. 5). Figure 6 shows that for $\alpha > \pi/4$, the Reynolds number has a minor effect on the pressure coefficient for convergent or divergent deflection. However, this figure depicts a negative (close to zero) value of C_p for parallel interaction. The higher values of C_p are reached for convergent interaction and the smallest values are obtained for parallel interaction for large Reynolds number. For each interaction, the pressure coefficient depends on the inclination and Reynolds number. The maximum values of pressure coefficient locations depend on inclination angles and interaction type due to the variation of the velocity components versus inclination of the jets for a given Reynolds number.

At the open boundary (exit), the atmospheric pressure is attained ($C_p=0.0$). In addition, for all cases, the minimum or maximum values correspond to the center eddies location.

3.3 Thermal Field

For $Re=50000$, the Fig. 7 shows the isotherms of each interaction type. For all cases, the isotherms closely follow the streamlines patterns and well-match with the flow field showing hot area near the impingement surface and development of thin thermal boundary layer. The maximum values reached near the wall at the stagnation points matching with the separation points of two contra-rotating eddies. The profiles are asymmetric for Parallel interaction.

3.4 Distribution of Nusselt Number

In order to evaluate the heat transfer characteristics of the coupled impingement cooling processes, the distribution of the local Nusselt number on the impingement surface is computed for all configurations. The local Nusselt number distribution over the impingement wall is defined as

(Eq. (16))

$$Nu(y) = -\left(\frac{w}{T_w - T_o}\right)\left(\frac{\partial T}{\partial x}\right)_{wall} \quad (16)$$

Effect of interaction type, inclination angle and Re are illustrated in Fig. 8. This figure confirms that the best distribution of local Nusselt number is obtained for the perpendicular interaction. The global convection process mainly depends on several parameters such as the jet exit Reynolds number and inclination angle of the oblique jet impingement.

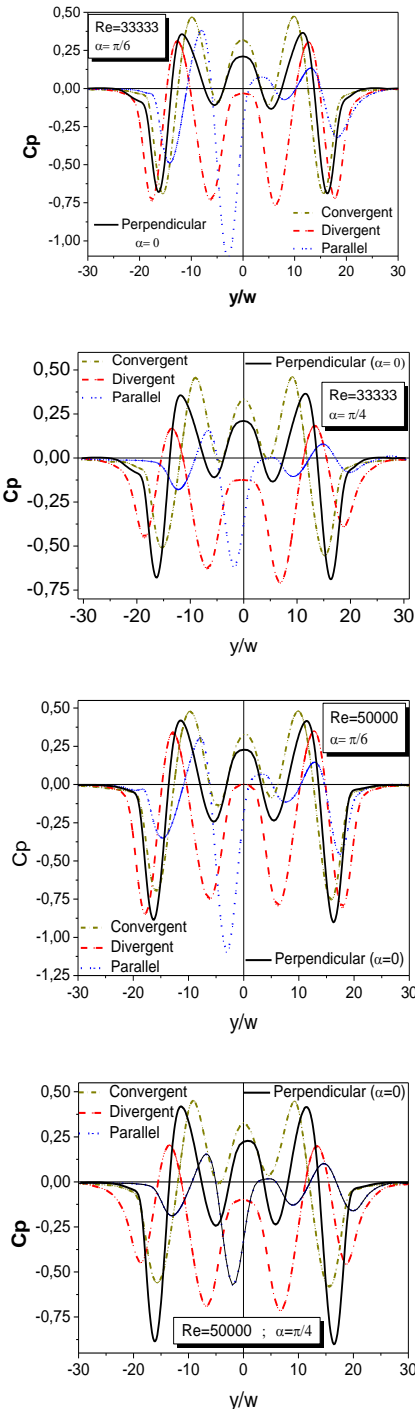


Fig. 5. Pressure coefficient ($0 \leq \alpha \leq \pi/4$).

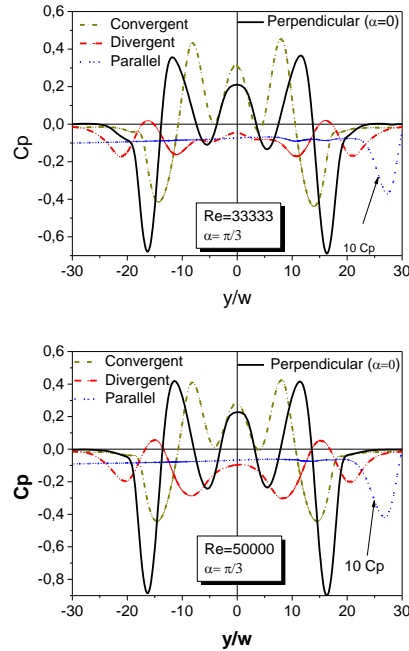


Fig. 6. Pressure coefficient ($\alpha > \pi/4$).

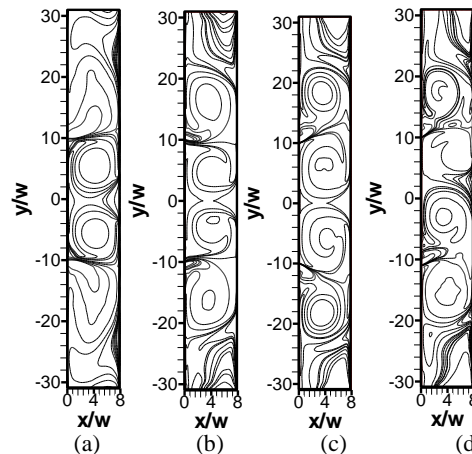


Fig. 7. Isotherms $Re=50000$, $H/w=20$, $D/w=8$ and $\alpha=\pi/6$ for oblique jets (a) Perpendicular, (b) Convergent, (c) Divergent and (d) Parallel.

For parallel interaction the two jets are completely deviated for $\alpha > \pi/4$, and practically does not reach the wall and its streamlines become progressively parallel to the wall. The flow is driven by a larger vertical velocity than that of perpendicular velocity.

In all cases, the maximum values of the Nusselt numbers are reached at the points where the value of C_p is zero and the minimum values of Nu occur at C_p maximum value point.

The average Nusselt number is deduced from the following equation (Eq. (17))

$$\overline{Nu} = \frac{1}{L} \int_{-L/2}^{L/2} Nu(y) dy \quad (17)$$

Figure 9 shows the average Nusselt number

evolution according Reynolds number for different angles. It may be concluded that:

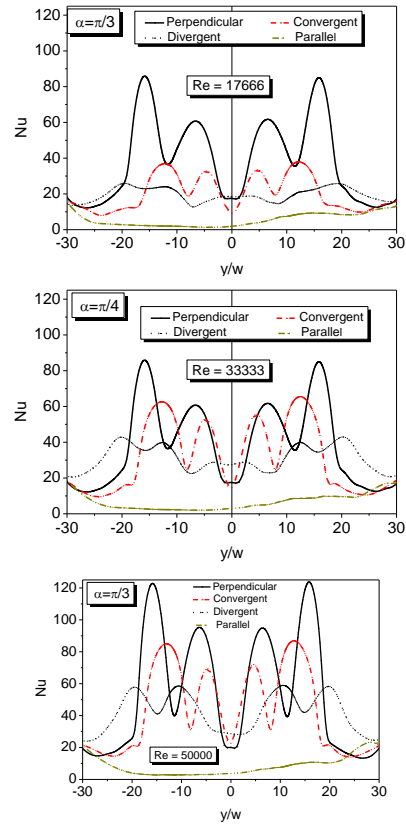
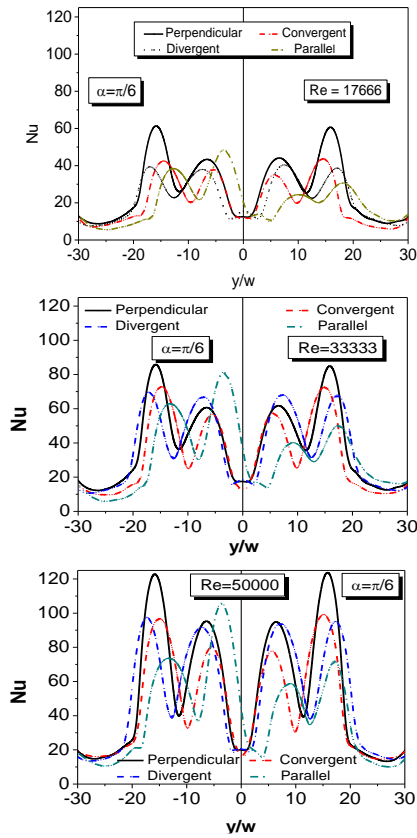


Fig. 8. Local Nusselt number along the heated wall. Effect of interaction type, inclination angle and Re, $H/w=20$, $D/w=8$.

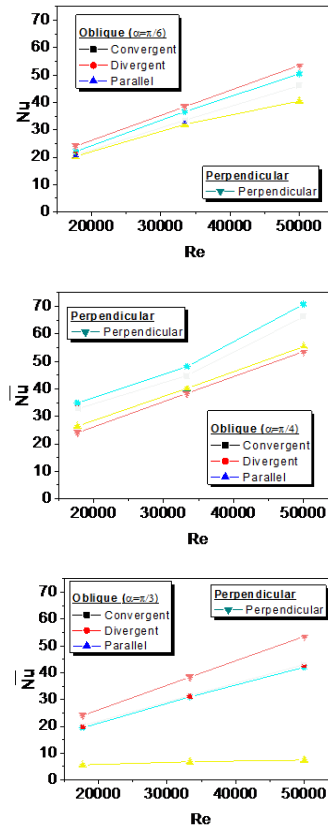
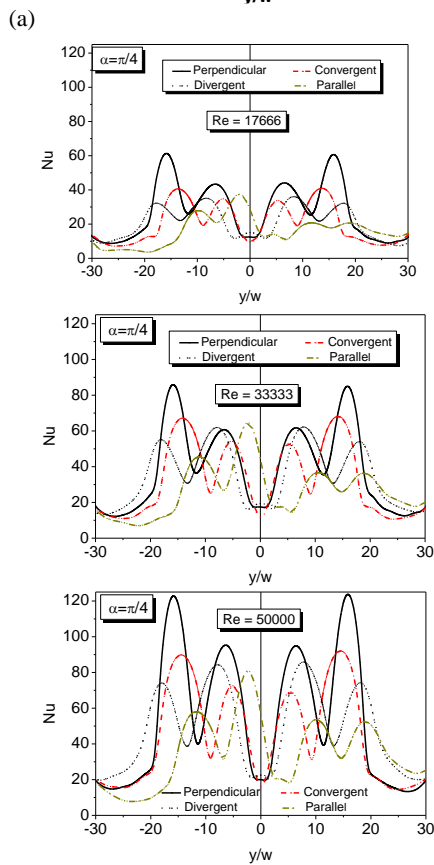


Fig. 9. Average Nusselt number along the heated wall for each interaction type, inclination angle and Reynolds number.

1- $\alpha < \pi/4$, the best heat transfer is obtained for perpendicular interaction and the lower heat transfer is obtained for parallel interaction. The heat transfer of divergent interaction is better than that of convergent interaction

2- $\alpha = \pi/4$, the best heat transfer is obtained for convergent interaction and the poorer heat transfer is obtained for parallel interaction. The heat transfer of divergent interaction exceeds that of convergent interaction

3- $\alpha > \pi/4$, the best heat transfer is obtained for perpendicular interaction and heat transfer of both convergent and divergent interaction is equivalent. The poorer heat transfer is obtained for parallel interaction

CONCLUSION

Analysis of the behavior of twin inclined jet impinging on a hot plate is performed in this paper. The location of stagnation point and maximum heat transfer depend on the inclination angle of the jet and it plays an important role for higher Reynolds number.

The skewed profiles of local heat transfer have been highlighted for jets Reynolds number in the range 17666 to 50000 and different orientations and inclinations of the jets (from normal 0° to $\pi/3$). The substantial variation of stagnation characteristic plays an important role in heat transfer. For $0 \leq \alpha \leq \pi/4$ symmetrical interactions (perpendicular, convergent or divergent), Reynolds number has a small effect on pressure coefficient, compared to parallel interaction. For parallel asymmetric interaction and $\alpha > \pi/4$, pressure coefficient is smaller than that of symmetrical interaction. The greatest values of C_p are obtained for convergent interaction and the least values for parallel interaction for large Reynolds number. For each interaction, the pressure coefficient depends on inclination and Reynolds number. The stagnation point's locations depend on inclination angles and interaction type induced by the variation of the velocity components versus inclination of the jets for a given Reynolds Number. The variation of local and average Nusselt number with Jet inclination, jet orientation and jet Reynolds are examined. The increase of Reynolds number induces an enhancement of heat transfer for each case. The average Nusselt number along the heated wall confirms that for the poorer heat transfer is obtained for all parallel interaction and the best heat transfer is obtained for perpendicular interaction excepting the case of $\alpha = \pi/4$ for which the diverging interaction is higher. For all case, heat transfer of diverging interaction exceeds that of converging interaction. As perspective, we will examine the horizontal movement of the fluid due to the inclination of the jets, which directly influences the displacement of the stagnation points and the associated heat transfer.

REFERENCES

Baydar, E. and Y. Ozmen (2005). An experimental

and numerical investigation on a confined impinging air jet at high Reynolds numbers. *Applied thermal engineering* 25(2), 409-421.

Beitelmal, A. H., M. A. Saad and C. D. Patel (2000). The effect of inclination on the heat transfer between a flat surface and an impinging two-dimensional air jet. *International Journal of Heat and Fluid Flow* 21(2), 156-163.

Benmouhoub, D. and A. Mataoui (2013). Turbulent heat transfer from a slot jet impinging on a flat plate. *Journal of heat transfer* 135(10), 102201.

Benmouhoub, D. and A. Mataoui (2015). Inclination of an impinging jet on a moving wall to control the stagnation point location. *International Journal of Thermal Sciences* 89, 294-304.

Bentarzi, F., A. Mataoui, N., Nouali and A. Terfous (2009). Numerical simulation of heat transfer in two turbulent plane jets impinging on a flat plate. *In ichmt digital library online*. Begel House Inc.

Bentarzi, F., M. Rebay and A. Mataoui (2014). Modelling of hydrodynamic and thermal behaviours in impinging twin-jets. *In ichmt digital library online*. Begel House Inc.

Buchlin, J. M. (2011). Convective Heat Transfer in Impinging - Gas - Jet Arrangements. *Journal of Applied Fluid Mechanics* 4(3).

Cho, H. H., K. M. Kim and J. Song (2011). Applications of impingement jet cooling systems. *Cooling Systems: Energy, Engineering and Applications, first ed.*, Nova Publishers, New York.

Cooper, D., Jackson, D. C., Launder, B. E., & Liao, G. X. (1993). Impinging jet studies for turbulence model assessment—I. Flow-field experiments. *International Journal of Heat and Mass Transfer*, 36(10), 2675-2684.

Craft, T. J., Graham, L. J. W., & Launder, B. E. (1993). Impinging jet studies for turbulence model assessment—II. An examination of the performance of four turbulence models. *International Journal of Heat and Mass Transfer*, 36(10), 2685-2697.

Craft, T. J., L. J. W. Graham and B. E. Launder (1993). Impinging jet studies for turbulence model assessment—II. An examination of the performance of four turbulence models. *International Journal of Heat and Mass Transfer* 36(10), 2685-2697.

Draksler, M. and B. Končar (2011). Analysis of heat transfer and flow characteristics in turbulent impinging jet. *Nuclear engineering and design* 241(4), 1248-1254.

- Gardon, R. and J. C. Akfirat (1966). Heat transfer characteristics of impinging two-dimensional air jets. *Journal of Heat Transfer* 88(1), 101-107.
- Germano, M., U. Piomelli, P. Moin and W. H. Cabot (1991). A dynamic subgrid-scale eddy viscosity model. *Physics of Fluids A: Fluid Dynamics* 3(7), 1760-1765.
- Goldstein, R. J. and M. E. Franchett (1988). Heat transfer from a flat surface to an oblique impinging jet. *ASME, Transactions, Journal of Heat Transfer* 110, 84-90.
- Hasegawa, H. and S. Kumagai (2008). Adaptive separation control system using vortex generator jets for time-varying flow. *Journal of Applied Fluid Mechanics* 1(2), 9-16.
- Jung, E. Y., S. H. Oh, D. H. Lee, K. M. Kim and H. H. Cho (2017). Effect of impingement jet on the full-coverage film cooling system with double layered wall. *Experimental Heat Transfer*, (just-accepted).
- Kito, M. (2012). Effect of inclination of impinging jets on flow and heat transfer characteristics. *Int. J. Science Eng. Invest* 1(9), 42-47.
- Koched, A., M. Pavageau and F. Aloui (2011). Vortex Structure in the Wall Region of an Impinging Plane Jet. *Journal of Applied Fluid Mechanics* 4(2).
- Lilly, D. K. (1992). A proposed modification of the Germano subgrid-scale closure method. *Physics of Fluids A: Fluid Dynamics* 4(3), 633-635.
- Livingood, J. N. and P. Hrycak (1973). Impingement heat transfer from turbulent air jets to flat plates: a literature survey
- Looney, M. K. and J. J. Walsh (1984). Mean-flow and turbulent characteristics of free and impinging jet flows. *Journal of Fluid Mechanics* 147, 397-429.
- Martin, H. (1977). Heat and mass transfer between impinging gas jets and solid surfaces. *Advances in heat transfer* 13, 1-60.
- Nouali, N. and A. Mataoui (2014). Analysis of steady turbulent triple jet flow with temperature difference. *Nuclear Engineering and Design* 280, 8-20.
- Oztop, H. F., Y. Varol, A. Koca, M. Firat, B. Turan and I. Metin (2011). Experimental investigation of cooling of heated circular disc using inclined circular jet. *International communications in heat and mass transfer* 38(7), 990-1001.
- Parida, P. R., S. V. Ekkad and K. Ngo (2011). Experimental and numerical investigation of confined oblique impingement configurations for high heat flux applications. *International Journal of Thermal Sciences* 50(6), 1037-1050.
- Rady, M. and E. Arquis (2006). Heat transfer enhancement of multiple impinging slot jets with symmetric exhaust ports and confinement surface protrusions. *Applied thermal engineering* 26(11), 1310-1319.
- Rathee, Y., B. R. Vinoth, P. K. Panigrahi and K. Muralidhar (2015). Imaging flow during impingement of differentially heated jets over a flat surface. *Nuclear Engineering and Design* 294, 1-15.
- Saad, N. R., S. Polat and W. J. M. Douglas (1992). Confined multiple impinging slot jets without crossflow effects. *International journal of heat and fluid flow* 13(1), 2-14.
- Seyedein, S. H., M. Hasan and A. S. Mujumdar (1995). Turbulent flow and heat transfer from confined multiple impinging slot jets. *Numerical Heat Transfer, Part A: Applications* 27(1), 35-51.
- Sharif, M. A. (2015). Heat transfer from an isothermally heated flat surface due to confined laminar twin oblique slot-jet impingement. *Journal of Thermal Science and Engineering Applications* 7(3), 03100
- Sharif, M. A. R. and A. Banerjee (2009). Numerical analysis of heat transfer due to confined slot-jet impingement on a moving plate. *Applied Thermal Engineering* 29(2), 532-540.
- Shukla, A. K. and A. Dewan (2017). Flow and thermal characteristics of jet impingement: comprehensive review. *International Journal of Heat And Technology* 35(1), 153-166.
- Smagorinsky, J. (1964). Some aspects of the general circulation. *Quarterly Journal of the Royal Meteorological Society* 90(383), 1-14.
- Sparrow, E. M. and B. J. Lovell (1980). Heat transfer characteristics of an obliquely impinging circular jet. *Journal of Heat Transfer* 102(2), 202-209.
- Tong, A. Y. (2003). On the impingement heat transfer of an oblique free surface plane jet. *International Journal of Heat and Mass Transfer* 46(11), 2077-2085.
- Wang, H., S. Lee and Y. A. Hassan (2016). Particle image velocimetry measurements of the flow in the converging region of two parallel jets. *Nuclear Engineering and Design* 306, 89-97.
- Wolfshtein, M. (1970). Some solutions of the plane turbulent impinging jet. *Journal of Basic Engineering* 92(4), 915-922.
- Zuckerman, N. and N. Lior (2005). Impingement heat transfer: correlations and numerical modeling. *Transactions of the ASME-C- Journal of Heat Transfer* 127(5), 544.
- Zuckerman, N. and N. Lior (2006). Jet impingement heat transfer: physics, correlations, and numerical modeling. *Advances in heat transfer* 39, 565-631.